

# Electrically tunable singular phase and Goos–Hänchen shifts in phase-change-material-based thin-film coatings as optical absorbers

Sreekanth, Kandammathe Valiyaveedu; Das, Chandreyee Manas; Medwal, Rohit; Mishra, Mayank; Ouyang, Qingling; Rawat, Rajdeep Singh; Yong, Ken-Tye; Singh, Ranjan

2021

Sreekanth, K. V., Das, C. M., Medwal, R., Mishra, M., Ouyang, Q., Rawat, R. S., Yong, K. & Singh, R. (2021). Electrically tunable singular phase and Goos–Hänchen shifts in phase-change-material-based thin-film coatings as optical absorbers. *Advanced Materials*, 33(15), 2006926-. <https://dx.doi.org/10.1002/adma.202006926>

<https://hdl.handle.net/10356/153514>

<https://doi.org/10.1002/adma.202006926>

---

This is the peer reviewed version of the following article: "Sreekanth, K. V., Das, C. M., Medwal, R., Mishra, M., Ouyang, Q., Rawat, R. S., . . . Singh, R. (2021). Electrically Tunable Singular Phase and Goos–Hänchen Shifts in Phase-Change-Material-Based Thin-Film Coatings as Optical Absorbers. *Advanced Materials*, 33(15), 2006926-, which has been published in final form at <https://doi.org/10.1002/adma.202006926>. This article may be used for non-commercial purposes in accordance with Wiley Terms and Conditions for Use of Self-Archived Versions.

# **Supporting Information: Electrically tunable singular phase and Goos-Hänchen shifts in phase change material based thin-film optical absorbers**

*Kandammathe Valiyaveedu Sreekanth, Chandreyee Manas Das, Rohit Medwal, Mayank Mishra, Qingling Ouyang, Rajdeep Singh Rawat, Ken-Tye Yong and Ranjan Singh\**

## **S1: Materials and Methods**

Sample fabrication: To fabricate thin-film absorbers, ~560 nm thick MMA copolymer from MICROCHEM (8.5MMAEL 11) was spin coated at 2600 rpm on 700  $\mu\text{m}$  thick Si substrates and 25 nm thick  $\text{Ge}_2\text{Sb}_2\text{Te}_5$  layer deposited glass substrates. The substrates were pre-cleaned using acetone, ethanol, and de-ionized water prior to spin coating and deposition.  $\text{Ge}_2\text{Sb}_2\text{Te}_5$  layer was deposited using RF magnetron sputtering. The distance between the substrate and target was kept 15 cm to achieve uniform deposition of thin films. The deposition was carried out at room temperature at a fixed RF power of 70 Watt under the high purity argon (99.999%) at deposition pressure of 10 mTorr.

Ellipsometer characterization: Variable-angle high-resolution spectroscopic ellipsometer (J. A. Woollam Co., Inc, V-VASE) was used to determine the thicknesses and the optical constants of MMA and GST layers. The ellipsometry parameters ( $\psi$  and  $\Delta$ ) as a function of incident angle and wavelength were acquired using the VASE ellipsometer with an angular resolution of  $1^\circ$  and a spectroscopic resolution of 2 nm.

Microheater fabrication and Temperature calibration: The metallic microheater was fabricated by optical lithography. Thin film of Al with thickness 200 nm was thermally deposited over the entire area and followed by lift-off process to leave behind the Al only in the patterned area. Thereafter, the microheater was subjected to the temperature calibration using Keithley 2450. A thermocouple was mounted at the center of the microheater and two probes were used to apply the DC current on the heating element. The temperature was recorded as a function of applied current.

Reflection measurements: The polarized reflectance spectra as a function of wavelength and incident angle were acquired using the variable-angle spectroscopic ellipsometer (J. A. Woollam Co., Inc, V-VASE) with a wavelength spectroscopic resolution of 2 nm and an angular resolution of 1°. The transmittance is zero for all wavelengths and angles. Since we are dealing with thin films, perfect light absorption corresponds to near zero reflectance. We consider  $R \leq 5 \times 10^{-4}$  to be zero reflectance since this is the noise limit of the detector which is determined by considering an incident *p*-polarized light on a non-chiral film and measuring the *s*-to-*p* reflectance which gives us the detector noise level for the parameters adopted in our measurements.

G-H shift measurements:

A schematic of home-built differential phase-sensitive setup used to measure G-H shift is shown in Fig. S1. As can be seen, we recorded the differential G-H shift between *p*- and *s*-polarized light. Since the point-of-darkness and phase singularity are obtained at 532 nm and 633 nm wavelengths, we used DPSS laser (532 nm) and He-Ne laser (632.8 nm) with a power of 5 mW as the excitation sources. The light from the source was separated into *p*- and *s*-polarized light using a polarized beam splitter (PBS). The *p*-polarized light travels along the original light path, while the *s*-polarized light travels in parallel with the *p*-polarized light by using two mirrors. Afterwards, the second mirror and PBS were used to change the path of *s*- polarized light to that of the *p*-polarized light. In this way, both *p*- and *s*- polarized light impinge onto the sample surface. A position sensitive detector (or lateral position sensor, Thorlabs, PDP90A) was used to collect the reflected light. The T-Cube controller is an accessory of the detector for recording the spot position. The overall measurement was operated by the LabVIEW program with a computer. We note that the chopper between the two PBS and mirrors has two functions: (i) to confirm only one beam of *s*- and *p*-polarized light can shine onto the sample surface at one time and (ii) the detector can collect

the signal of  $p$ - and  $s$ -polarized light alternately when the chopper is rotated. The position data of  $p$ - and  $s$ -polarized light was used to obtain the targeted results of the differential G-H shift. The sample was immobilized on a rotating translation stage. The position of the reflected  $p$ - and  $s$ -polarized light as a function of incident angle was recorded using the position sensitive detector with a data acquisition card for further processing.

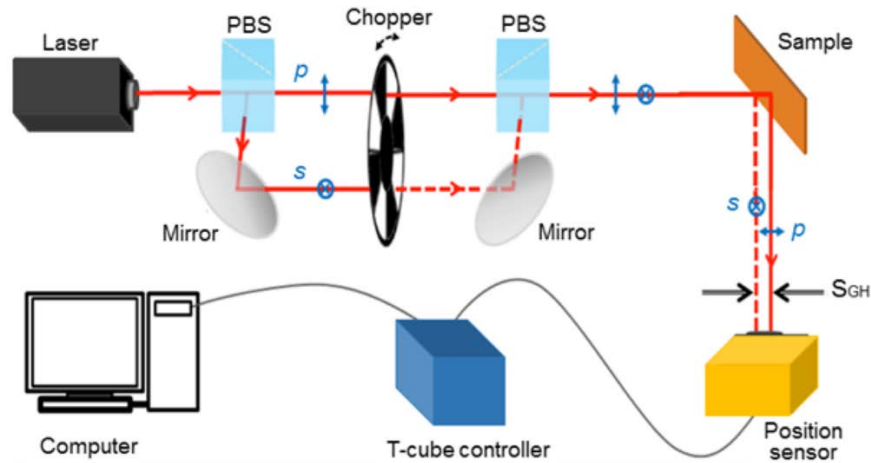


**Figure S1** Schematic representation of the G-H shift measurement setup.

To prove that slight shift of Brewster angle towards higher incident angle is attribute to the surface roughness of MMA layer due to laser exposure, we measured the singular phase and G-H shift by replacing MMA layer with  $\text{SiO}_2$ . For this purpose, we deposited  $\sim 700$  nm thick  $\text{SiO}_2$  layer on Si substrate and measured ellipsometry parameters. As shown in Fig. S2a,  $\text{SiO}_2/\text{Si}$  stack shows  $p$ -polarized Brewster angle at  $75^\circ$  and 532 nm. As a result, minimum  $\psi$  value with abrupt phase change is obtained at 532 nm. We then performed the G-H shift measurement using  $\text{SiO}_2/\text{Si}$  sample and 532 nm laser (Power=5 mW). As shown in Fig. S2b, maximum G-H shift is obtained at  $76^\circ$ . It indicates that the Brewster angle is just  $1^\circ$  shifted with laser exposure on  $\text{SiO}_2/\text{Si}$  sample. However, an angle shift of  $3^\circ$  is obtained for MMA/Si sample at 532 nm. Therefore, it can be concluded that the observed increased angle shift is attributed to the increase in surface roughness

of the transparent dielectric layer (MMA and SiO<sub>2</sub>) due to laser exposure. Since polymer layer (MMA) surface roughness increases largely than dielectric layer (SiO<sub>2</sub>) with laser exposure, higher angle shift is obtained for MMA/Si stack. We note that the realized maximum G-H shift (18 μm) for SiO<sub>2</sub>/Si stack is lower compared to MMA/Si stack at 532 nm. This is because the abrupt phase change recorded at 532 nm is smaller due to higher  $\psi$  value (2.15°).

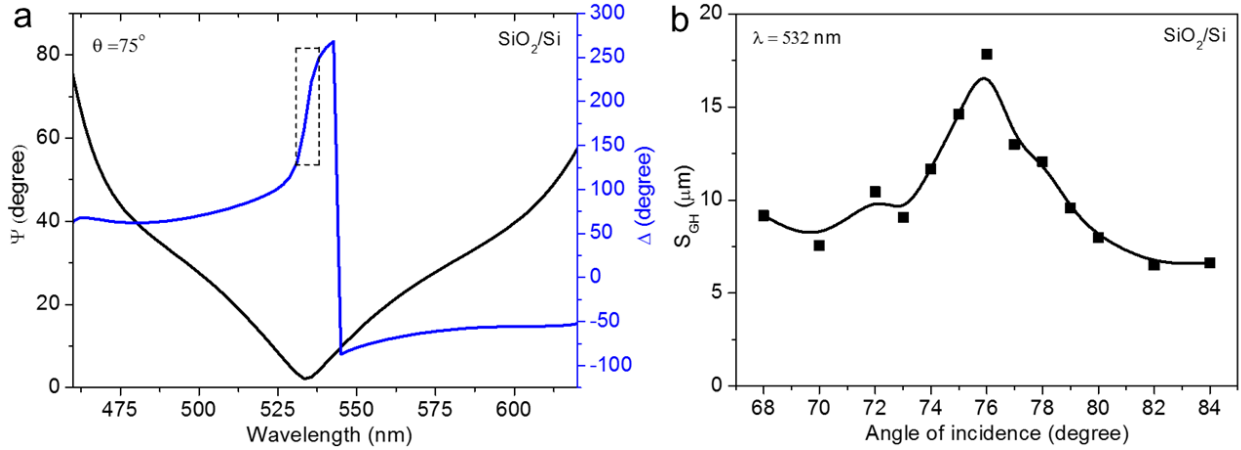


**Figure S2 (a)** Measured ellipsometry parameters of SiO<sub>2</sub>/Si stack at 75°, **(b)** Measured G-H shift as a function of incident angle at 532 nm.

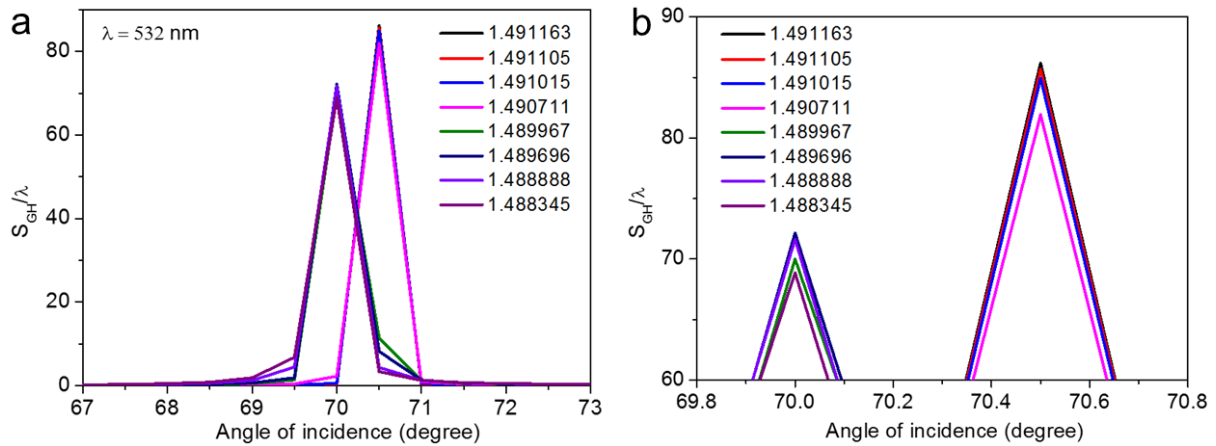


**Figure S3 (a)** Calculated tunable G-H shifts at 532 nm with change in refractive index of MMA. **(b)** Zoomed part of (a).

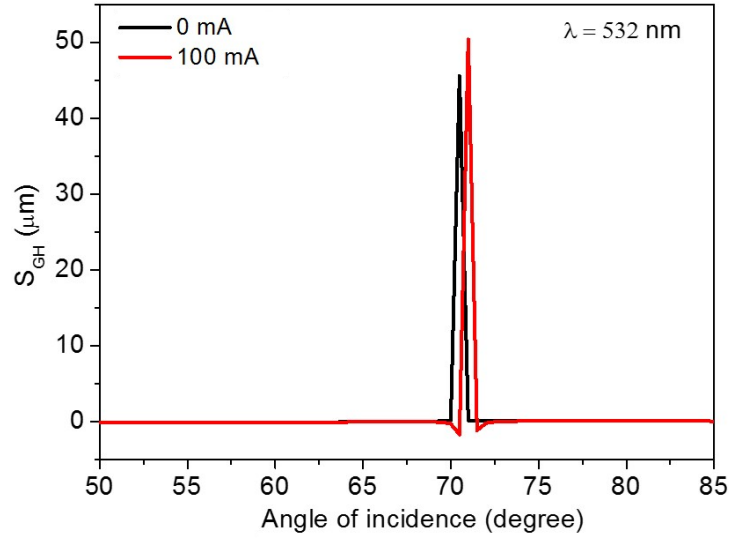


**Figure S4** Calculated G-H shifts of Si/MMA at 532 nm when applied current is 0 mA and 100 mA. A maximum thickness expansion of 3 nm and a slight surface roughness increase of 0.25 nm are obtained when the current is increased from 0 to 100 mA. Here, we compare the simulated G-H shifts obtained at 532 nm for 0 mA and 100 mA (with expanded thickness and change in refractive index of MMA layer) and found that G-H shifts considerably vary near the Brewster angle.

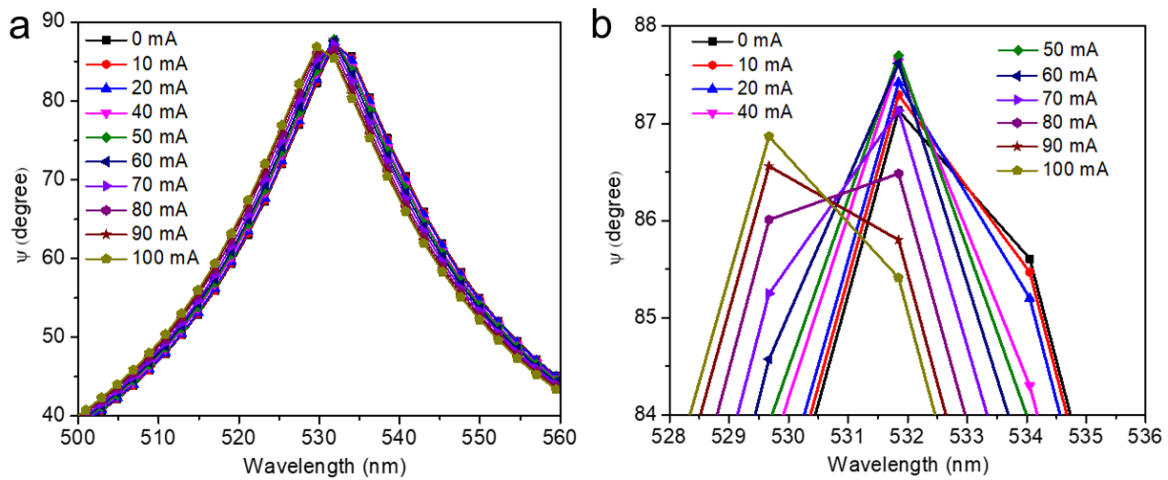


**Figure S5 (a)** Experimentally obtained ellipsometry parameter,  $\psi$  of Si/MMA stack at s-polarized Brewster angle ( $70^\circ$ ) with varying current. (b) Zoomed part of (a).

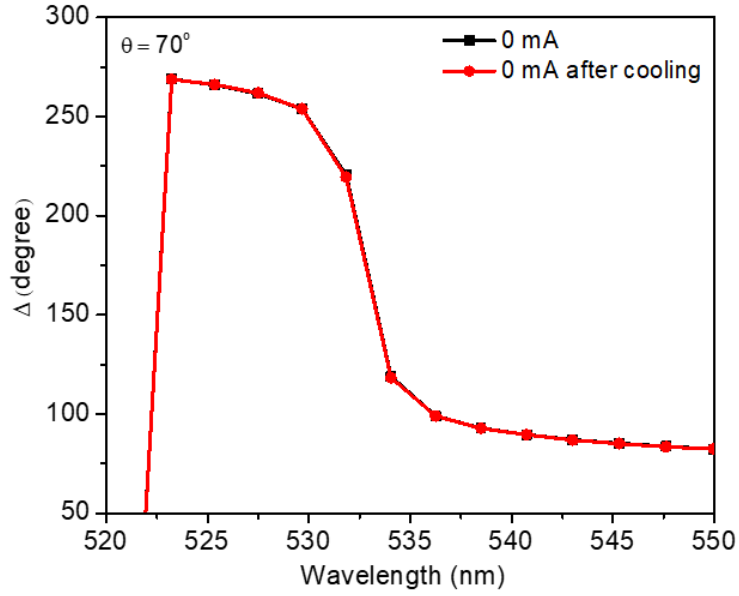


**Figure S6** Demonstration of reversible phase shift. Measured ellipsometry parameters,  $\Delta$  of Si/MMA stack in the forward and reverse direction at 0 mA (RT).

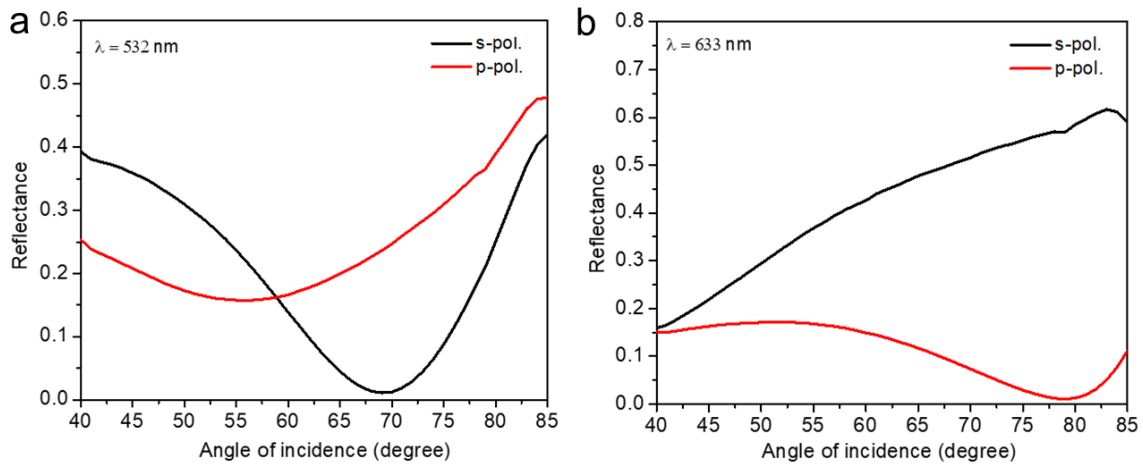


**Figure S7** Experimental demonstration of GBA in glass/GST (amorphous)/MMA stack. Angular reflectance spectrum for *s*- and *p*-polarizations (a) at 532 nm and (b) 633 nm.

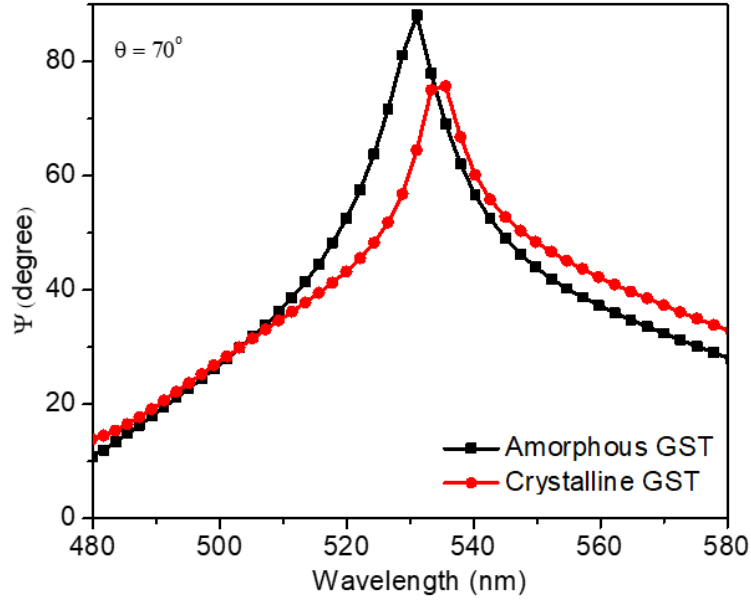


**Figure S8** Measured ellipsometry parameter,  $\psi$  of glass/GST/MMA at  $s$ -polarized Brewster angle ( $70^\circ$ ) for amorphous and crystalline phase of GST.

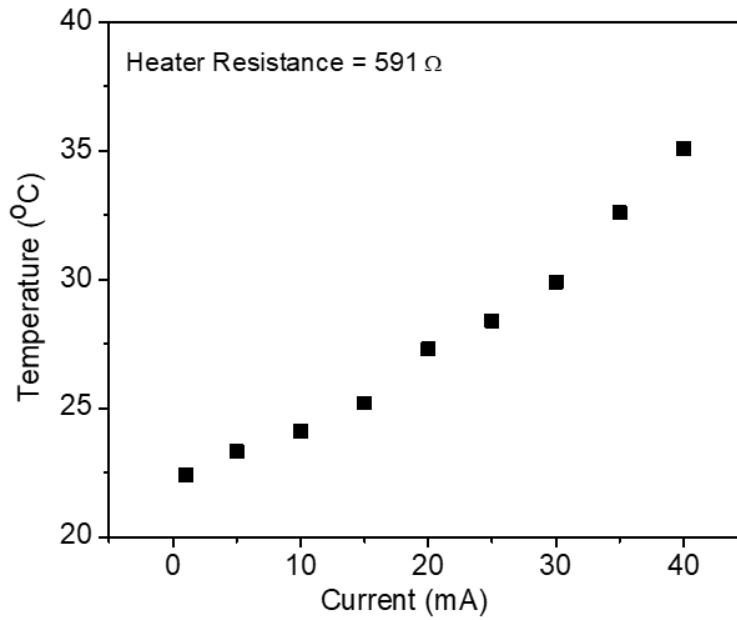


**Figure S9** Temperature calibration of microheater integrated glass/GST/MMA thin film absorber. Measured heater resistance at RT is  $591\Omega$ .

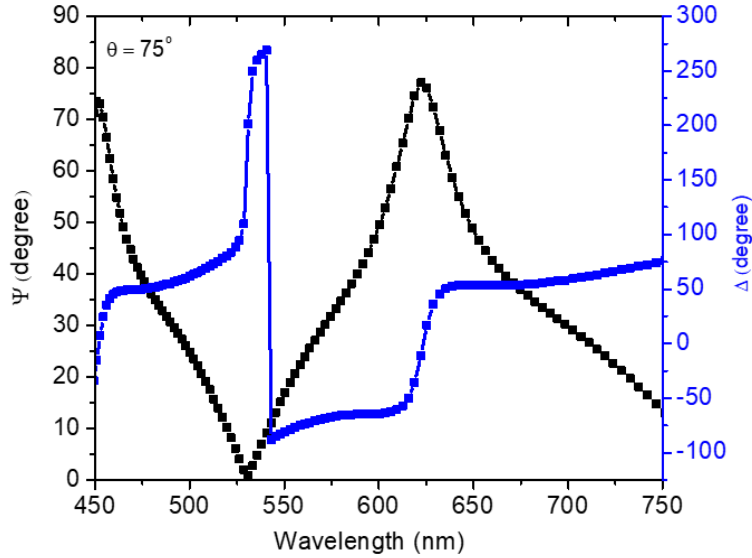


**Figure S10** Measured ellipsometry parameters,  $\psi$  and  $\Delta$  for glass/GST (amorphous)/MMA cavity at  $p$ -polarized Brewster angle of  $75^\circ$ .

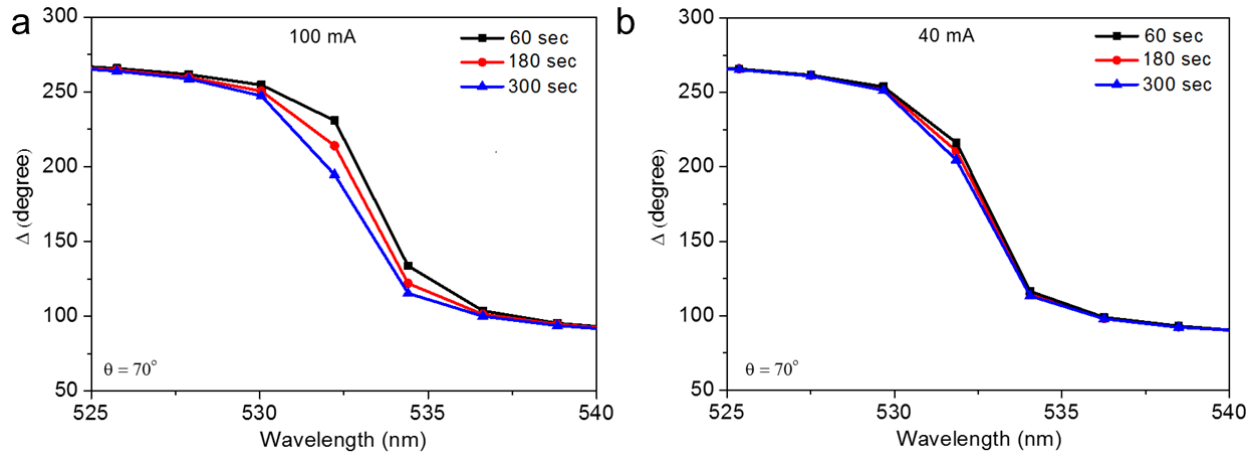


**Figure S11** Tuning of phase at the Brewster angle with increasing time when current (a) 100 mA and (b) 40 mA. Since the phase and G-H shift tuning mechanism of the proposed Si/MMA is based on the temperature induced volatile refractive index change of MMA, it is a slow process. In fact, the G-H shift tunability depends on temperature. That means, the modulation speed increases with increasing temperature or current. The modulation time of the G-H shift is of the order of hundreds of seconds below 60 mA and few seconds above 60 mA. It is clear that the phase modulation time is faster and slower at 100 mA and 40 mA, respectively.